

Distributed Control of Spacecraft Formation via Cyclic Pursuit: Theory and Experiments

Jaime L. Ramirez, Marco Pavone, Emilio Frazzoli, David W. Miller

Abstract—In this paper we study distributed control policies for spacecraft formations that draw inspiration from the simple idea of cyclic pursuit. First, we extend existing cyclic-pursuit control laws devised for single-integrator models in two dimensions to the case of double-integrator models in three dimensions. In particular, we develop control laws that only require relative measurements of position and velocity with respect to the two leading neighbors in the ring topology of cyclic pursuit, and allow the spacecraft to converge to a variety of symmetric formations, including evenly spaced circular formations and evenly spaced Archimedes' spirals. Second, we discuss potential applications, including spacecraft coordination for interferometric imaging and convergence to zero-effort orbits. Finally, we present and discuss experimental results obtained by implementing the aforementioned control laws on three nanospacecraft on board the International Space Station.

I. INTRODUCTION

In recent years, the idea of *distributing* the functionalities of a complex agent among multiple simpler and cooperative agents is attracting an ever increasing interest. In fact, multi-agent systems present several advantages. For instance, the intrinsic parallelism of a multi-agent system provides robustness to failures of single agents, and in many cases can guarantee better time efficiency. Moreover, it is possible to reduce the total implementation and operation cost, increase reactivity and system reliability, and add flexibility and modularity to monolithic approaches.

In this context, geometric pattern formation problems are of particular interest, especially for their connection to formation flight. Indeed, the idea of distributing the functionality of a large spacecraft among smaller, cooperative spacecraft flying in formation has been considered for numerous space missions. For instance, a cluster of spacecraft flying in formation for high-resolution, synthetic-aperture imaging can act as a sparse aperture with an effective dimension larger than the one that can be achieved by a single, larger satellite [1].

Recently, many distributed control strategies have been proposed for convergence to geometric patterns. Justh *et al.* [2] presented two strategies to achieve, respectively, rectilinear and circle formation; their approach, however, requires all-to-all communication among agents. Olfati-Saber *et al.* [3] and Leonard *et al.* [4] used potential function theory to prescribe flocking behavior. Lin *et al.* [5] exploited cyclic pursuit (where each agent i pursues the next $i + 1$, modulo

n) to achieve alignment among agents, while Marshall *et al.* in [6] and in [7] extended the classic cyclic pursuit to a system of wheeled vehicles, each subject to a single non-holonomic constraint, and studied the possible equilibrium formations and their stability. Paley *et al.* [8] introduced control strategies which extend previous research to formations of particles around convex curves.

In [9], we developed distributed control policies for convergence to symmetric formations. The key features of our approach are global stability and the capability to achieve with the same simple control law different formations, namely rendez-vous to a single point, circles or logarithmic spirals in two dimensions. Our approach generalizes the classic cyclic pursuit strategy by letting each of the n mobile agents, modeled as single integrators, pursue its leading neighbor along the line of sight *rotated* by a common offset angle α . Such approach is attractive since it is distributed and requires the minimum number of communication links (n links for n agents) to achieve a formation.

The contribution of this paper is threefold. First, in Section III, we extend the distributed control laws in [9], that we devised for single-integrator models in two dimensions, to the case of double-integrator models in three dimensions. In particular, we develop control laws that only require *relative* measurements of position and velocity with respect to the two leading neighbors in the ring topology of cyclic pursuit, and allow the agents to converge from *any* initial condition (except for a set of measure zero) to a single point, an evenly-spaced circular formation, an evenly-spaced logarithmic spiral formation or an evenly-spaced Archimedes' spiral formation, depending on some tunable control parameters. Control laws that only rely on relative measurements are indeed of critical importance in deep-space missions, where global measurements may not be available. A similar set of results has recently appeared in the two-part paper [10], [11]. However, the control laws proposed in [10], [11] require a global measurement of velocity; moreover, they do not provide Archimedes' spiral formations, which, as we will argue in this paper, are among the most useful symmetric formations for applications. Second, in Section IV, we discuss potential applications, including spacecraft coordination for interferometric imaging and convergence to zero-effort orbits. Finally, in Section V, we present and discuss experimental results obtained by implementing the proposed control laws on three nanospacecraft on board the International Space Station (ISS).

Jaime L. Ramirez, Marco Pavone, Emilio Frazzoli and David W. Miller are with the Department of Aeronautics and Astronautics, Massachusetts Institute of Technology, Cambridge. {ramirez, pavone, frazzoli, millerd}@mit.edu.

II. BACKGROUND

In this section, we provide some definitions and results from matrix theory. Moreover, we briefly review the distributed control laws presented in [9].

A. Kronecker Product

Let A and B be $m \times n$ and $p \times q$ matrices, respectively. Then, the Kronecker product $A \otimes B$ of A and B is the $mp \times nq$ matrix

$$A \otimes B = \begin{bmatrix} a_{11}B & \dots & a_{1n}B \\ \vdots & & \vdots \\ a_{m1}B & \dots & a_{mn}B \end{bmatrix}.$$

If λ_A is an eigenvalue of A with associated eigenvector ν_A and λ_B is an eigenvalue of B with associated eigenvector ν_B , then $\lambda_A \lambda_B$ is an eigenvalue of $A \otimes B$ with associated eigenvector $\nu_A \otimes \nu_B$. Moreover, the following property holds: $(A \otimes B)(C \otimes D) = AC \otimes BD$, where A, B, C and D are matrices with appropriate dimensions.

B. Determinant of Block Matrices

If A, B, C and D are matrices of size $n \times n$ and $AC = CA$, then

$$\det \left(\begin{bmatrix} A & B \\ C & D \end{bmatrix} \right) = \det(AD - CB). \quad (1)$$

C. Rotation Matrices

A rotation matrix is a real square matrix whose transpose is equal to its inverse and whose determinant is +1. The eigenvalues of a rotation matrix in two dimensions are $e^{\pm j\theta}$, where θ is the magnitude of the rotation and j is the imaginary unit. The eigenvalues of a rotation matrix in three dimensions are 1, and $e^{\pm j\theta}$, where θ is the magnitude of the rotation about the rotation axis; for a rotation about the axis $(0, 0, 1)^T$, the corresponding eigenvectors are $(0, 0, 1)^T, (1, +i, 0)^T, (1, -i, 0)^T$.

D. Cyclic Pursuit for Single Integrators

Let there be n ordered mobile agents in the plane, their positions at time $t \geq 0$ denoted $x_i(t) = [x_{i,1}(t), x_{i,2}(t)]^T \in \mathbb{R}^2$, $i \in \{1, 2, \dots, n\}$, where agent i pursues the next $i+1$ modulo n . The kinematics of each agent is described by a simple integrator [9]:

$$\begin{aligned} \dot{x}_i &= u_i, \\ u_i &= R(\theta)(x_{i+1} - x_i), \end{aligned} \quad (2)$$

where $R(\theta)$, $\theta \in [-\pi, \pi)$, is the rotation matrix:

$$R(\theta) = \begin{pmatrix} \cos \theta & \sin \theta \\ -\sin \theta & \cos \theta \end{pmatrix}.$$

Let $x = [x_1^T, x_2^T, \dots, x_n^T]^T$; the dynamics of the overall system can be written in compact form as

$$\dot{x} = (L \otimes R(\theta)) x,$$

where L is the circulant matrix

$$L = \begin{bmatrix} -1 & 1 & 0 & \dots & 0 \\ 0 & -1 & 1 & \dots & 0 \\ \vdots & & & & \vdots \\ 1 & 0 & 0 & \dots & -1 \end{bmatrix}.$$

The eigenvalues of matrix L are $e^{2\pi k j/n} - 1$, $k \in \{1, \dots, n\}$. Then, by the properties of the Kronecker product, the $2n$ eigenvalues of $L \otimes R(\theta)$ are $(e^{2\pi k j/n} - 1)e^{\pm j\theta}$, $k \in \{1, \dots, n\}$. The following is proven in [9]:

- Theorem 1:* Two eigenvalues of $L \otimes R(\theta)$ are zero, and
- 1) if $0 \leq |\theta| < \pi/n$, all non-zero eigenvalues lie in the open left-half complex plane;
 - 2) if $|\theta| = \pi/n$, two non-zero eigenvalues lie on the imaginary axis, while all other non-zero eigenvalues lie in the open left-half complex plane;
 - 3) if $\pi/n < |\theta| < 2\pi/n$, two non-zero eigenvalues lie in the open right-half complex plane, while all other non-zero eigenvalues lie in the open left-half complex plane;

Moreover, it is possible to prove (see [9]) that the matrix $L \otimes R(\theta)$ is diagonalizable for all values of θ . Then, it is straightforward to show that agents starting at any initial condition (except for a set of measure zero) in \mathbb{R}^{2n} and evolving under (2) exponentially converge:

- 1) if $0 \leq |\theta| < \pi/n$, to a single limit point, namely their initial center of mass;
- 2) if $|\theta| = \pi/n$, to an evenly spaced circle formation;
- 3) if $\pi/n < |\theta| < 2\pi/n$, to an evenly spaced logarithmic spiral formation.

The previous results can be easily generalized to the three-dimensional case. Indeed, let $x_i(t) = [x_{i,1}(t), x_{i,2}(t), x_{i,3}(t)]^T \in \mathbb{R}^3$ be the position at time $t \geq 0$ of the i th agent, $i \in \{1, 2, \dots, n\}$, and let $x = [x_1^T, x_2^T, \dots, x_n^T]^T$. Moreover, let $R(\theta)^1$ be the rotation matrix in three dimensions with rotation angle $\theta \in [-\pi, \pi)$ and rotation axis $(0, 0, 1)^T$. The dynamics of the overall system in three dimensions become

$$\dot{x} = (L \otimes R(\theta)) x. \quad (3)$$

By the properties of the Kronecker product, the $3n$ eigenvalues of $L \otimes R(\theta)$ are:

$$\begin{aligned} \lambda_k &= e^{2\pi k j/n} - 1 && \text{for } k = 1, \dots, n, \\ \lambda_k &= e^{2\pi(k-n)j/n+j\theta} - e^{j\theta} && \text{for } k = n+1, \dots, 2n, \\ \lambda_k &= e^{2\pi(k-2n)j/n-j\theta} - e^{-j\theta} && \text{for } k = 2n+1, \dots, 3n. \end{aligned} \quad (4)$$

Note that for $k \in \{1, \dots, n-1\}$ the eigenvalues λ_k lie in the open left-half complex plane, for $k = n$ we have $\lambda_n = 0$, and for $k \in \{n+1, \dots, 3n\}$ the eigenvalues λ_k are the same as those in Theorem 1. Then it is possible to state for the three

¹With a slight abuse of notation we use the same symbol for rotation matrices in two and three dimensions; the meaning will be clear from the context.

dimensional case a theorem virtually identical to Theorem 1 (the only difference is that now there are three zero eigenvalues). Moreover, the matrix $L \otimes R(\theta)$ is diagonalizable for all values of θ [14]. Then, it is straightforward to show that agents starting at any initial condition (except for a set of measure zero) in \mathbb{R}^{3n} and evolving under (2) exponentially converge to a single limit point if $0 \leq |\theta| < \pi/n$, to an evenly spaced circle formation if $|\theta| = \pi/n$, and to an evenly spaced logarithmic spiral formation if $\pi/n < |\theta| < 2\pi/n$.

III. DYNAMIC CYCLIC PURSUIT

In this section, we extend the previous cyclic pursuit control laws to double integrators; i.e., we consider a *dynamic* model for the agents. We first present a control law that requires each agent to be able to measure its global velocity; then, we design a control law that only requires *relative* measurements of position and velocity. As before, let $x_i(t) = [x_{i,1}(t), x_{i,2}(t), x_{i,3}(t)]^T \in \mathbb{R}^3$ be the position at time $t \geq 0$ of the i th agent, $i \in \{1, 2, \dots, n\}$, and let $x = [x_1^T, x_2^T, \dots, x_n^T]^T$. Moreover, let $R(\theta)$ be the rotation matrix in three dimensions with rotation angle $\theta \in [-\pi, \pi)$ and rotation axis $(0, 0, 1)^T$. The dynamics of each agent are now described by a double-integrator model:

$$\ddot{x}_i = u_i. \quad (5)$$

A. Dynamic Cyclic Pursuit with Reference Coordinate Frame

Consider the following feedback control law

$$u_i = k_d R(\theta) (x_{i+1} - x_i) + R(\theta) (\dot{x}_{i+1} - \dot{x}_i) - k_d \dot{x}_i, \quad (6)$$

where k_d is a positive constant. Then, the overall dynamics of the n agents are described by:

$$\begin{bmatrix} \dot{x} \\ \ddot{x} \end{bmatrix} = \begin{bmatrix} 0 & I_{3n} \\ k_d A(\theta) & A(\theta) - k_d I_{3n} \end{bmatrix} x \doteq C(\theta) x \quad (7)$$

where $A(\theta) \doteq L \otimes R(\theta)$, I_{3n} is the $3n$ -by- $3n$ identity matrix, and L is the *circulant* matrix defined previously. The following theorem characterizes eigenvalues and eigenvectors of $C(\theta)$.

Theorem 2: Assume that $-k_d$ is not an eigenvalue of $A(\theta)$. The eigenvalues of the state matrix $C(\theta)$ in Eq. (7) are the union of:

- the $3n$ eigenvalues of $A(\theta)$,
- $-k_d$, with multiplicity $3n$.

In other words, $\lambda(C(\theta)) = \lambda(A(\theta)) \cup \{-k_d\}$. Moreover, the eigenvector of $C(\theta)$ corresponding to the k th eigenvalue $\lambda_k \in \lambda(A(\theta))$, $k = 1, \dots, 3n$, is:

$$\nu_k \doteq \begin{bmatrix} \nu_{k,1} \\ \nu_{k,2} \end{bmatrix} = \begin{bmatrix} \mu_k \\ \lambda_k \mu_k \end{bmatrix}, \quad k = 1, \dots, 3n,$$

where μ_k is the eigenvector of $A(\theta)$ corresponding to λ_k . The $3n$ (independent) eigenvectors corresponding to the eigenvalue $-k_d$ (that has multiplicity $3n$) are

$$\nu_k \doteq \begin{bmatrix} \nu_{k,1} \\ \nu_{k,2} \end{bmatrix} = \begin{bmatrix} -k_d^{-1} e_{k-3n} \\ e_{k-3n} \end{bmatrix}, \quad k = 3n + 1, \dots, 6n,$$

where e_j is the j th vector of the canonical basis in \mathbb{R}^{3n} .

Proof: First, we compute the eigenvalues of $C(\theta)$. The eigenvalues of $C(\theta)$ are, by definition, solutions to the characteristic equation:

$$0 = \det \begin{bmatrix} \lambda I_{3n} & -I_{3n} \\ -k_d A(\theta) & \lambda I_{3n} - (A(\theta) - k_d I_{3n}) \end{bmatrix}.$$

By using the result in Eq.(1), we obtain

$$\begin{aligned} 0 &= \det(\lambda^2 I_{3n} - \lambda(A(\theta) - k_d I_{3n}) - k_d A(\theta)) \\ &= \det((\lambda + k_d) I_{3n}) \det(\lambda I_{3n} - A(\theta)). \end{aligned}$$

Thus, the eigenvalues of $C(\theta)$ must satisfy $0 = \det((\lambda + k_d) I_{3n})$ and $0 = \det(\lambda I_{3n} - A(\theta))$; thus, the first part of the claim is proved.

By definition, the eigenvector $[\nu_{k,1}^T, \nu_{k,2}^T]^T$ corresponding to the eigenvalue λ_k , $k = 1, \dots, 6n$, satisfies the eigenvalue equation:

$$\begin{aligned} \lambda_k \begin{bmatrix} \nu_{k,1} \\ \nu_{k,2} \end{bmatrix} &= \begin{bmatrix} 0 & I_{3n} \\ k_d A(\theta) & A(\theta) - k_d I_{3n} \end{bmatrix} \begin{bmatrix} \nu_{k,1} \\ \nu_{k,2} \end{bmatrix} \\ &= \begin{bmatrix} \nu_{k,2} \\ k_d A(\theta) \nu_{k,1} + A(\theta) \nu_{k,2} - k_d \nu_{k,2} \end{bmatrix}. \end{aligned}$$

Thus, we obtain

$$\begin{aligned} \lambda_k \nu_{k,1} &= \nu_{k,2}, \\ \lambda_k \nu_{k,2} &= k_d A(\theta) \nu_{k,1} + A(\theta) \nu_{k,2} - k_d \nu_{k,2}, \end{aligned}$$

and therefore

$$\lambda_k (k_d + \lambda_k) \nu_{k,1} = (k_d + \lambda_k) A(\theta) \nu_{k,1}. \quad (8)$$

If $\lambda_k = -k_d$, then we have $3n$ eigenvectors given by $[-k_d^{-1} e_j, e_j]^T$, $j = \{1, \dots, 3n\}$. If, instead, $\lambda_k \in \lambda(A(\theta))$ (note that by assumption $-k_d \notin \lambda(A(\theta))$), we obtain from Eq. (8)

$$\lambda_k \nu_{k,1} = A(\theta) \nu_{k,1},$$

and we obtain the claim. \blacksquare

Theorem 3: Assume that $-k_d$ is not an eigenvalue of $A(\theta)$. Consider the vector field defined by equation (6). Then, agents' positions starting at any initial condition (except for a set of measure zero) in \mathbb{R}^{3n} and evolving under (6) exponentially converge to:

- 1) if $0 \leq |\theta| < \pi/n$, to a single limit point, namely their initial center of mass;
- 2) if $|\theta| = \pi/n$, to an evenly spaced circle formation;
- 3) if $\pi/n < |\theta| < 2\pi/n$, to an evenly spaced logarithmic spiral formation.

Proof: As a consequence of Theorem 2, the eigenvectors of $C(\theta)$ are linearly independent. Indeed, the eigenvectors ν_k for $k = 1, \dots, 3n$ are linearly independent since the vectors μ_k are (as proven in [9]), moreover, the eigenvectors ν_k for $k = 3n + 1, \dots, 6n$ are clearly linearly independent; since, by assumption, $-k_d \notin \lambda(A(\theta))$, the claim then follows from the fact that eigenvectors corresponding to different eigenvalues are linearly independent.

Then, from the discussion in Section II about the eigenvalues of $L \otimes R(\theta)$ and from Theorem 2, the general solution can be written as

$$\begin{aligned} \begin{bmatrix} x(t) \\ \dot{x}(t) \end{bmatrix} &= \sum_{k=2}^q \sum_{j=1}^{m_k} \alpha_{kj} e^{t\lambda_k} \nu_{jk} + x_G d_G^1 + y_G d_G^2 + z_G d_G^3 \\ &= \sum_{k=2}^q \sum_{j=1}^{m_k} \alpha_{kj} \begin{bmatrix} e^{t\lambda_k} \mu_{jk} \\ \lambda_k e^{t\lambda_k} \mu_{jk} \end{bmatrix} \\ &\quad + x_G d_G^1 + y_G d_G^2 + z_G d_G^3, \end{aligned}$$

where q is the number of distinct eigenvalues, m_k is the multiplicity of eigenvalue λ_k , α_{kj} are constants, d_G^i are constant vectors in \mathbb{R}^{6n} , and $(x_G, y_G, z_G)^T$ is another vector of constants. Then, from the discussion in Section II about the eigenvalues of $L \otimes R(\theta)$ and from Theorem 2, if $0 \leq |\theta| < \pi/n$, all non-zero eigenvalues are in the open left-half complex plane and the agents will converge to a single limit point; if $|\theta| = \pi/n$, two non-zero eigenvalues are on the imaginary axis and all other non-zero eigenvalues are in the open left-half complex plane, and the agents will converge to an evenly spaced circle formation; finally, if $\pi/n < |\theta| < 2\pi/n$, two non-zero eigenvalues are in the open right-half complex plane and all other non-zero eigenvalues are in the open left-half complex plane, and the agents will converge to an evenly spaced logarithmic spiral formation. ■

B. Control Law with only Relative Information

Consider the following feedback control law:

$$\begin{aligned} u_i &= k_1 R^2(\theta) \left((x_{i+2} - x_{i+1}) - (x_{i+1} - x_i) \right) \\ &\quad + k_2 R(\theta) (\dot{x}_{i+1} - \dot{x}_i), \end{aligned} \quad (9)$$

where k_1 and k_2 are two real constants (not necessarily positive). In this case, each agent needs only to measure its *relative* position with respect to the positions of agents $i+1$ and $i+2$, and its *relative* velocity with respect to the velocity of agent $i+1$.

It is possible to verify that

$$L^2 = \begin{bmatrix} 1 & -2 & 1 & 0 & \dots & 0 \\ 0 & 1 & -2 & 1 & \dots & 0 \\ \vdots & & & & & \vdots \\ -2 & 1 & 0 & \dots & \dots & 1 \end{bmatrix}$$

Then, the overall dynamics of the n agents can be written in compact form as

$$\begin{bmatrix} \dot{x} \\ \ddot{x} \end{bmatrix} = \begin{bmatrix} 0 & I_{3n} \\ k_1 L^2 \otimes R^2(\theta) & k_2 (L \otimes R(\theta)) \end{bmatrix} x \doteq F(\theta) x. \quad (10)$$

Denote, as before, $A(\theta) = L \otimes R(\theta)$, and define

$$\beta_{\pm} \doteq \frac{k_2}{2} \pm \sqrt{\left(\frac{k_2}{2}\right)^2 + k_1}. \quad (11)$$

The following theorem characterizes eigenvalues and eigenvectors of $F(\theta)$.

Theorem 4: Assume that $\beta_{\pm} \neq 0$. The eigenvalues of the state matrix $F(\theta)$ in Eq. (10) are the union of:

- the $3n$ eigenvalues of $A(\theta)$, each one multiplied by β_+ ,
- the $3n$ eigenvalues of $A(\theta)$, each one multiplied by β_- .

In other words, $\lambda(F(\theta)) = \beta_+ \lambda(A(\theta)) \cup \beta_- \lambda(A(\theta))$. Moreover, the eigenvector of $F(\theta)$ corresponding to the k th eigenvalue $\lambda_k \in \beta_+ \lambda(A(\theta))$, $k = 1, \dots, 3n$, is:

$$\nu_k \doteq \begin{bmatrix} \nu_{k,1} \\ \nu_{k,2} \end{bmatrix} = \begin{bmatrix} \mu_k \\ \lambda_k \mu_k \end{bmatrix}, \quad k = 1, \dots, 3n,$$

where μ_k is the eigenvector of $A(\theta)$ corresponding to the eigenvalue λ_k/β_+ . Similarly, the eigenvector corresponding to the k th eigenvalue $\lambda_{3n+k} \in \beta_- \lambda(A(\theta))$, $k = 1, \dots, 3n$, is:

$$\nu_{3n+k} \doteq \begin{bmatrix} \nu_{3n+k,1} \\ \nu_{3n+k,2} \end{bmatrix} = \begin{bmatrix} \mu_k \\ \lambda_k \mu_k \end{bmatrix}, \quad k = 1, \dots, 3n,$$

where μ_k is the eigenvector of $A(\theta)$ corresponding to the eigenvalue λ_k/β_- .

Proof: First, we compute the eigenvalues of $F(\theta)$. Notice that $L^2 \otimes R^2(\theta) = (L \otimes R(\theta))^2 = A^2(\theta)$. The eigenvalues of $F(\theta)$ are, by definition, solutions to the characteristic equation:

$$0 = \det \left(\begin{bmatrix} \lambda I_{3n} & -I_{3n} \\ -k_1 A^2(\theta) & \lambda I_{3n} - k_2 A(\theta) \end{bmatrix} \right).$$

Using the result in Eq. (1) we have that

$$\begin{aligned} 0 &= \det (\lambda^2 I_{3n} - k_2 \lambda A(\theta) - k_1 A^2(\theta)) \\ &= \det ((\lambda I_{3n} - \beta_+ A(\theta)) (\lambda I_{3n} - \beta_- A(\theta))) \end{aligned}$$

Then, the first part of the claim is proven.

By definition, the eigenvector $[\nu_{k,1} \ \nu_{k,2}]^T$ corresponding to the eigenvalue λ_k , $k = 1, \dots, 6n$, satisfies the eigenvalue equation:

$$\begin{aligned} \lambda_k \begin{bmatrix} \nu_{k,1} \\ \nu_{k,2} \end{bmatrix} &= \begin{bmatrix} 0 & I_{3n} \\ k_1 A^2(\theta) & k_2 A(\theta) \end{bmatrix} \begin{bmatrix} \nu_{k,1} \\ \nu_{k,2} \end{bmatrix} \\ &= \begin{bmatrix} \nu_{k,2} \\ k_1 A^2(\theta) \nu_{k,1} + k_2 A(\theta) \nu_{k,2} \end{bmatrix} \end{aligned}$$

Thus, we obtain

$$\begin{aligned} \lambda_k \nu_{k,1} &= \nu_{k,2}, \\ \lambda_k \nu_{k,2} &= k_1 A^2(\theta) \nu_{k,1} + k_2 A(\theta) \nu_{k,2}, \end{aligned}$$

and therefore,

$$\lambda_k^2 \nu_{k,1} = k_1 A^2(\theta) \nu_{k,1} + k_2 A(\theta) \lambda_k \nu_{k,1},$$

which can be rewritten as

$$(\lambda_k I_{3n} - \beta_+ A(\theta)) (\lambda_k I_{3n} - \beta_- A(\theta)) \nu_{k,1} = 0. \quad (12)$$

Therefore, if $\lambda_k \in \beta_+ \lambda(A(\theta))$, the above equation is satisfied by letting $\nu_{k,1}$ be equal to μ_k , in fact (notice that μ_k

is the eigenvector of $A(\theta)$ corresponding to the eigenvalue λ_k/β_+ and that $\beta_+ \neq 0$):

$$\lambda_k \nu_{k,1} = \frac{\lambda_k}{\beta_+} \beta_+ \mu_k = \beta_+ A(\theta) \mu_k = \beta_+ A(\theta) \nu_{k,1}.$$

By appropriately choosing k_1 , k_2 and θ , it is possible to obtain a variety of formations. Here we focus only on circular formations and Archimedes' spiral formations, which are probably among the most important symmetric formation for applications. In particular, Archimedes' spiral formations are useful for the solution of the coverage path-planning problem, where the objective is to ensure that at least one agent eventually moves to within a given distance from any point in the target environment. More applications will be discussed in Section IV.

Theorem 5: Let $k_2 = 2 \cos(\pi/2n)$ and $k_1 = -(k_2/2)^2 - \sin^2(\pi/2n)$. Moreover, assume that $\theta = \pi/2n$; then, the system converges to an evenly spaced circular formation whose geometric center has constant velocity.

Proof: The proof of this theorem is very similar to the proof of Theorem 7 and it is omitted in the interest of brevity; we refer the interest reader to [14].

Next we show how to choose k_1 , k_2 and θ to achieve Archimedes' spiral formations. We start with the following lemma:

Lemma 6: Let $k_1 = -(k_2/2)^2$ and assume $\theta = \pi/n$. Then,

$$w_k \doteq \begin{bmatrix} 0_{3n \times 1} \\ \mu_k \end{bmatrix}$$

is a generalized eigenvector for the eigenvalue λ_k/β .

Proof: The proof reduces to a straightforward verification. ■

Theorem 7: Let $k_1 = -(k_2/2)^2$, and assume $k_2 > 0$ and $\theta = \pi/n$. Then, the system converges to Archimedes' spirals whose geometric center has constant velocity.

Proof: In this case we have $\beta_- = \beta_+ \in \mathbb{R}$, and thus $\lambda_k = \lambda_{k+3n}$ for $k = 1, \dots, 3n$; as a consequence, the eigenvalues of $F(\theta)$ are $\beta \lambda(A(\theta))$ with algebraic multiplicity 2 and geometric multiplicity 1. The solution to the dynamic system can be written as:

$$x(t) = \sum_{k=1}^q \sum_{j=1}^{m_{\lambda_k}} c_{kj} e^{t\lambda_k} \nu_{jk} + \sum_{k=1}^q \sum_{j=1}^{m_{\lambda_k}} d_{kj} e^{t\lambda_k} (t\nu_{jk} + w_{jk})$$

where w_{jk} are the generalized eigenvectors of $F(\theta)$ defined in Lemma 6. By Theorem 4 and Lemma 6, after transients, we obtain

$$\begin{bmatrix} x(t) \\ \dot{x}(t) \end{bmatrix} = \begin{bmatrix} x_G \\ \dot{x}_G \end{bmatrix} + t \begin{bmatrix} \dot{x}_G \\ 0_{3n \times 1} \end{bmatrix} + d_1 \begin{bmatrix} 0_{3n \times 1} \\ w_{dom}^1 \end{bmatrix} + d_2 \begin{bmatrix} 0_{3n \times 1} \\ w_{dom}^2 \end{bmatrix} + (c_1 + d_1 t) \begin{bmatrix} w_{dom}^1 \\ -\omega w_{dom}^2 \end{bmatrix} + (c_2 + d_2 t) \begin{bmatrix} w_{dom}^2 \\ \omega w_{dom}^1 \end{bmatrix}$$

where x_G and \dot{x}_G are the initial position and velocity of the center of the formation, where $\omega = 2 \sin(\frac{\pi}{n})$, and where

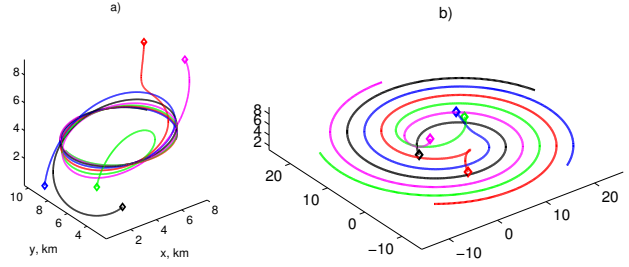


Fig. 1. Convergence from random initial conditions to symmetric formations using only relative navigation. Left: Circular trajectories, Right: Archimedes' spiral.

w_{dom}^i are the eigenfunctions

$$\begin{aligned} w_{dom}^1 &= [\cos(\omega t + \delta_i), \sin(\omega t + \delta_i)]_{i=1, \dots, n}, \\ w_{dom}^2 &= [\sin(\omega t + \delta_i), -\cos(\omega t + \delta_i)]_{i=1, \dots, n}. \end{aligned}$$

Then agents will perform spiraling trajectories; the radial growth rate is the constant $\sqrt{d_1 + d_2}$ and the center of the formation moves with constant velocity \dot{x}_G defined by the initial condition. ■

IV. APPLICATIONS

In the past few years, cyclic pursuit has received considerable attention in the control community; however, to the best of our knowledge, no practical application has been proposed for which cyclic pursuit is a particularly effective control strategy. In this section, we propose an application domain in which cyclic pursuit is indeed an ideal candidate control law.

Interferometric imaging, i.e., image reconstruction from interferometric patterns, is an application of formation flight that has been devised and studied for missions such as NASA's TPF and ESA's Darwin [12]. The general problem of interferometric imaging consists of performing measurements in a way that enough information about the frequency content of the image is obtained. A heuristic solution to this coverage problem is represented by *Archimedes' spirals* [13]. The application of the described cyclic pursuit algorithm to the so-called uv plane coverage is inherently appropriate given the fact that the frequency plane coverage problem is independent of the global location of the spacecraft, and it lies only on the space of relative positions. Additionally, missions like TPF and Darwin consider locations far out of the reach of GPS signals and are expected to rely on relative measurements to perform reconfigurations and observation maneuvers. Figure 1 shows simulated trajectories resulting from the application of control law (9); the initial positions are random inside a volume of $(10km)^3$. In the first case the vehicles converge to circular trajectories, while in the second case the vehicles converge to Archimedes' spirals. The inertial frame for the plots is the geometric center of the configuration.

The previous control laws can also be modified to obtain elliptical trajectories; the key idea is to use similarity transformations, in particular to replace $R(\theta)$ with $TR(\theta)T^{-1}$,



Fig. 2. Picture of the three SPHERES spacecraft performing a test on board the ISS (Fotocredit: NASA-SSL).

where T is an invertible 3×3 matrix. In the Clohessy-Wiltshire model, that describes the motion of a satellite about a reference circular orbit, elliptical trajectories are closed *zero-effort* trajectories. By adopting the aforementioned similarity transformation approach, it is possible to let the system globally converge to such *zero-effort* trajectories. The details are subject of ongoing research and will be discussed in a forthcoming paper.

V. EXPERIMENTS ON BOARD THE ISS

We tested the previous control laws on the SPHERES testbed on board the International Space Station. SPHERES is an experimental testbed consisting of a group of small vehicles with the basic functionalities of a satellite [15]. Their propulsion system uses compressed CO_2 gas, and their metrology system is “GPS-like.” Each vehicle has a local estimator that calculates a global estimate of the state from measurements of ultrasound pulses. The system uses a single TDMA based RF channel to communicate its state to neighboring spacecraft. Figure 2 shows a picture of three SPHERES spacecraft on board the ISS.

The dynamics of each spacecraft are well approximated by a double integrator. For the tests presented in this section, we used a velocity-tracking control law to track the velocity profile in (2). Convergence to evenly spaced circular trajectories with a *prescribed* radius is achieved by making the rotation angle θ *dynamic*, in particular we let:

$$\theta_i = \pi/n + k_\theta(r - \|x_{i+1} - x_i\|),$$

where $r > 0$ and $k_\theta > 0$; note that the rotation angles are potentially different across the agents. Intuitively, if the agents are “close to each other” with respect to r , they will spiral out since $\theta_i > \pi/n$; conversely, if they are “far from each other” with respect to r , they will spiral in since $\theta_i < \pi/n$. It is easy to see that a formation whereby all agents move on a circle of radius $r/(2 \sin(\pi/n))$ around the (fixed) center of mass of the group, with all agents being evenly spaced on the circle, is a *relative* equilibrium for the system. The local stability of such equilibrium is formally demonstrated in [14].

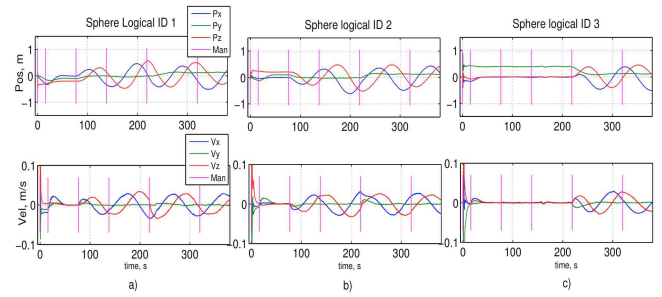


Fig. 3. Experimental results: position and velocity versus time for each spacecraft.

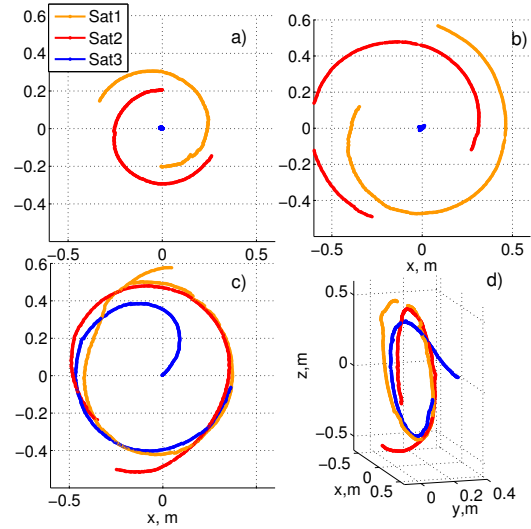


Fig. 4. Experimental results: a) rotation in the x - z plane; b) convergence to a circle with larger radius; c) the third spacecraft joins the formation; d) 3D plot of third maneuver.

The test comprised the following series of maneuvers, with the initial conditions being $x_1 = [0, -0.1, -0.2]^T$, $x_2 = [0, 0.1, 0.2]^T$, $x_3 = [0, 4, 0]^T$ and zero velocity (with respect to the ISS):

- 1) two spacecraft perform a rotation maneuver in the x - z plane;
- 2) a change in the desired radius is commanded and the spacecraft spiral out to achieve a circular formation with larger radius;
- 3) a third spacecraft joins the formation and the system reconfigures into a three-spacecraft evenly-spaced circular formation.

The aim is to test actual convergence to evenly-spaced circular formations and robustness to changes in the number of agents. Figure 3 shows spacecraft’s global position and velocity (with respect to the ISS); figure 4 shows the trajectories performed by the spacecraft. Experimental results (see in particular Fig. 4) demonstrate the effectiveness of the proposed cyclic-pursuit controller. Videos of experimental results can be accessed at <http://ssl.mit.edu/spheres/video/CyclicPursuit>. More experimental results can be found in [14].

VI. CONCLUSIONS

In this paper we studied distributed control policies for spacecraft formation that draw inspiration from the simple idea of cyclic pursuit. We discussed potential applications and we presented experimental results. This paper leaves numerous important extensions open for further research. First, all the algorithms that we proposed are synchronous: we plan to devise algorithms that are amenable to asynchronous implementation. Second, we envision to study the problem of convergence to symmetric formations in presence of actuator saturation. Finally, to further assess closed-loop robustness, we plan to perform additional tests on board the ISS.

ACKNOWLEDGEMENTS

The authors would like to thank the SPHERES team at the Space Systems Laboratory at MIT, especially Dr. Alvar Sanz-Otero and Christopher Mandy, for facilitating the implementation on board the ISS and for their support in obtaining the experimental results.

This work was supported in part by NSF grants #0705451 and #0705453. Any opinions, findings, and conclusions or recommendations expressed in this publication are those of the authors and do not necessarily reflect the views of the supporting organizations.

REFERENCES

- [1] Kang, W., Sparks, A., and Banda, S., *Coordinated Control Of Multi-satellite Systems*, Journal of Guidance, Control, and Dynamics. Vol. 24, No. 2, 2001, pp. 360-368.
- [2] E. W. Justh and P. S. Krishnaprasad, *Steering laws and continuum models for planar formations*, Proc. 42nd IEEE Conf. Decision and Control, Hawaii, USA, Dec. 2003, pp. 3609 - 3614.
- [3] R. O. Saber and R. M. Murray, *Flocking with Obstacle Avoidance: Cooperation with Limited Communication in Mobile Networks*, Proc. of the 42nd IEEE Conference on Decision and Control, Hawaii, USA, Dec. 2003, pp. 2022 - 2028.
- [4] N. Leonard and E. Friorelli, *Virtual leaders, artificial potentials and coordinated control of groups*, Proc. 39th IEEE Conference on Decision and Control, Orlando, FL, 2001, pp. 2968 - 2973.
- [5] Z. Lin, M. Broucke, and B. Francis, *Local control strategies for groups of mobile autonomous agents*, IEEE Trans. on Automatic Control, 49(4):622-629, 2004.
- [6] J. A. Marshall, M. E. Broucke and B. A. Francis, *Formations of Vehicles in Cyclic Pursuit*, IEEE Transactions On Automatic Control, Vol. 49, No. 11, November 2004.
- [7] J. A. Marshall, M. E. Broucke and B. A. Francis, *Pursuit Formations of Unicycles*, Automatica, vol. 41, no. 12, December 2005.
- [8] D. A. Paley, N. Leonard, R. Sepulchre, *Stabilization of symmetric formations to motion around convex loops*. Systems & Control letters, v.57, 2008. pp. 209-215
- [9] Pavone, M., Frazzoli, E. *Decentralized policies for geometric pattern formation and path coverage*. Journal of Dynamic Systems, Measurement, and Control. v.129, Issue 5, 2007 pp. 633-643
- [10] Ren W. *Collective motion from consensus with Cartesian coordinate coupling - Part I: Single-integrator kinematics*. Proc. 47th IEEE Conference on Decision and Control, Cancun, Mexico, Dec. 2008, pp. 1006 - 1011.
- [11] Ren W. *Collective motion from consensus with Cartesian coordinate coupling - Part II: Double-integrator dynamics*. Proc. 47th IEEE Conference on Decision and Control, Cancun, Mexico, Dec. 2008, pp. 1012 - 1017.
- [12] C.V.M. Fridlund, *Darwin The Infrared Space Interferometry Mission*, Advances in Space Research, ESTEC, Noordwijk, The Netherlands. v. 34, n.3, 2004, pp. 613-617
- [13] Chakravorty, S., Ramirez, J., Chakravorty, S. *On the Fuel Optimal of Multispacecraft Interferometric Imaging systems*, Journal of Guidance, Control and Dynamics, v.30 n.1, Jan-Feb 2007. pp 227-236.
- [14] J. Ramirez, M. Pavone, E. Frazzoli, D. Miller. *Spacecraft Decentralized Control based on Cyclic-Pursuit Strategies* (In preparation).
- [15] <http://ssl.mit.edu/spheres/>